Stress-induced activation of the AMP-activated protein kinase in the freeze-tolerant frog *Rana sylvatica* ☆

Mark H. Rider [a],*, Nusrat Hussain [a], Sandrine Horman [a],
Stephen M. Dilworth [b], Kenneth B. Storey [c]

[a] *Hormone and Metabolic Research Unit, Christian de Duve Institute of Cellular Pathology, University of Louvain Medical School, Avenue Hippocrate, 75, B-1200 Brussels, Belgium*
[b] *Tumour Cell Biology, Department of Metabolic Medicine, Imperial College Faculty of Medicine, Hammersmith Hospital, Du Cane Road, London W12 0NN, UK*
[c] *Institute of Biochemistry, Department of Biology, Carleton University, 1125 Colonel By Drive, Ottawa, Ont., Canada K1S 5B6*

Abstract

Survival in the frozen state depends on biochemical adaptations that deal with multiple stresses on cells including long-term ischaemia and tissue dehydration. We investigated whether the AMP-activated protein kinase (AMPK) could play a regulatory role in the metabolic re-sculpting that occurs during freezing. AMPK activity and the phosphorylation state of translation factors were measured in liver and skeletal muscle of wood frogs (*Rana sylvatica*) subjected to anoxia, dehydration, freezing, and thawing after freezing. AMPK activity was increased 2-fold in livers of frozen frogs compared with the controls whereas in skeletal muscle, AMPK activity increased 2.5-, 4.5- and 3-fold in dehydrated, frozen and frozen/thawed animals, respectively. Immunoblotting with phospho-specific antibodies revealed an increase in the phosphorylation state of eukaryotic elongation factor-2 at the inactivating Thr56 site in livers from frozen frogs and in skeletal muscles of anoxic frogs. No change in phosphorylation state of eukaryotic initiation factor-2α at the inactivating Ser51 site was seen in the tissues under any of the stress conditions. Surprisingly, ribosomal protein S6 phosphorylation was increased 2-fold in livers from frozen frogs and 10-fold in skeletal muscle from frozen/thawed animals. However, no change in translation capacity was detected in cell-free translation assays with skeletal muscle extracts under any of the experimental conditions. The changes in phosphorylation state of translation factors are discussed in relation to the control of protein synthesis and stress-induced AMPK activation.
© 2006 Elsevier Inc. All rights reserved.

Keywords: Metabolic rate depression; AMPK; Energy stress; mTOR; eEF2; eEF2K; p70S6K; 4E-BP1; Ribosomal protein S6

The present study explores the responses of AMPK and multiple downstream targets of its action in liver and muscle of wood frogs in order to determine the role of this central regulator of cellular energy metabolism in mediating metabolic events that aid natural freeze tolerance. In parallel, we analyzed changes in the activity (phosphorylation states) of various translation factors in order to assess global protein synthesis activity. Our analysis includes the effects of freezing and thawing on these parameters as well as the effects of two component stresses of freezing, anoxia and dehydration.

Freezing is one of the most serious environmental stresses faced by living organisms and is lethal for the vast majority. However, a variety of organisms that live in cold environments have perfected mechanisms for freeze tolerance. Freezing survival depends on adaptations that address the multiple stresses caused by freezing, such as potential physical damage to tissues by ice crystals, dehydration and cell volume reduction due to the exit of cellular water into extracellular ice, and long-term anoxia/ischaemia caused by the freezing of blood plasma. Biochemical adaptations that support natural freeze tolerance include the accumulation of high levels of carbohydrate cryoprotectants, the production of ice-nucleating proteins, defenses against anoxia and oxidative stresses, alterations in gene expression, and metabolic rate depression [39,40,43]. Carbohydrate metabolism and energy production are central issues during freezing. All organs must deal with long-term anoxia/ischaemia, relying on endogenous glycogen reserves and anaerobic glycolysis (ending in lactate) to sustain cell viability. Glycogen reserves are also mobilized to synthesize the high concentrations of cryoprotectants that are needed to regulate cell volume and protect macromolecules during the freeze. For example, in wood frogs (*Rana sylvatica*), freezing triggers a massive hyperglycemia that raises glucose in core organs to levels as high as 150–300 mM compared with concentrations around 5 mM in unfrozen controls [38]. This requires several alterations to the normally tight homeostatic control of glucose levels that is typically displayed by vertebrates.

The AMP-activated protein kinase (AMPK) is a highly conserved eukaryotic serine/threonine protein kinase that acts not only as a sensor of cellular energy status but also plays a critical role in systemic energy balance [14,20,21]. AMPK is a heterotrimer consisting of a catalytic α subunit and two regulatory subunits, β and γ. Each subunit has multiple isoforms (α1, α2, β1,

β2, γ1, γ2, γ3) giving twelve possible combinations of holoenzyme with different tissue distributions and subcellular localizations. AMPK is activated via phosphorylation by upstream AMPK kinases (AMP-KKs) [20,47]. The activating phosphorylation site is Thr172 in the T-loop of the α-subunit and phosphorylation at this site is both sufficient and necessary for AMPK activation. Upstream activating kinases phosphorylating Thr172 have been identified as the Peutz-Jeghers Syndrome protein LKB1 and calcium/calmodulin-dependent protein kinases [20,47]. AMPK is activated by changes in the intracellular AMP:ATP ratio, as occurs under anoxia or other stresses, and the binding of AMP to the γ-subunits is thought to somehow induce a conformational change that allows α-subunit Thr172 phosphorylation by LKB1. Once activated, AMPK inhibits ATP-consuming processes and stimulates ATP-producing pathways [14,21,20]. For example, fatty acid synthesis is inhibited via the AMPK-mediated phosphorylation and inactivation of acetyl-CoA carboxylase (ACC). As a consequence, malonyl-CoA concentrations fall which stimulates fatty acid oxidation, thereby contributing to the maintenance of intracellular ATP levels. In addition, AMPK activation stimulates glycolysis by increasing glucose uptake in skeletal muscle [30] and heart [36] and by activating heart 6-phosphofructo-2-kinase [27].

Protein synthesis and the Na^+/K^+-ATPase are the two most prominent consumers of ATP in mammalian cells [7,46]. Peptide chain elongation consumes at least 4 equivalents of ATP for each peptide bond synthesized and is inhibited via the phosphorylation of eukaryotic elongation factor-2 (eEF2) at Thr56 by a highly specific Ca^{2+} and calmodulin-dependent kinase called eEF2 kinase (eEF2K) [32]. AMPK activation leads to the inhibition of eEF2 by phosphorylating and activating eEF2K [5,16,17]. This promotes inhibition of energy-expensive protein synthesis under low cellular energy conditions. Control of eEF2K is also exerted by a variety of other upstream protein kinases including p70S6K [44]. p70S6K phosphorylates and inactivates eEF2K and the mammalian target of rapamycin (mTOR) lies upstream of p70S6K and has been proposed to act as an ATP sensor in cells [11]. Thus, a reduction in ATP levels and a decrease in mTOR signalling could lead to an increase in eEF2K activity and the subsequent phosphorylation of eEF2. In addition, AMPK activation inhibits p70S6K [3,12,22] possibly via phosphorylation of the tuberous sclerosis complex (TSC1–TSC2) [19]. TSC2 acts as a GAP (GTPase activating protein) for the small GTPase Rheb (Ras-homologue enriched in brain) thereby inactivating
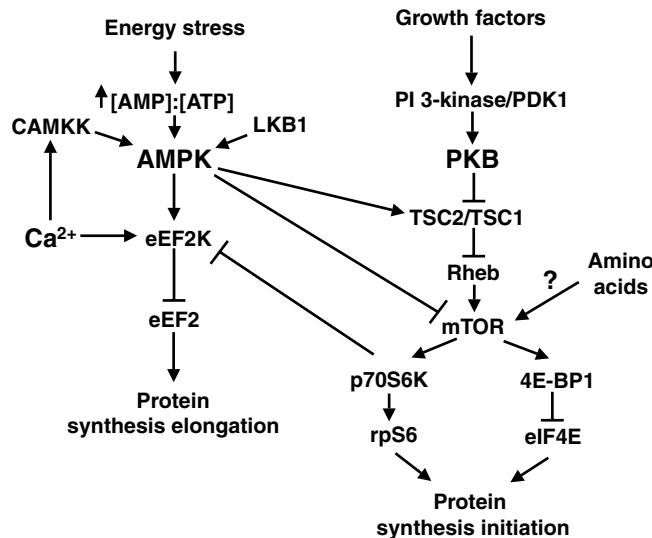
Fig. 1. Potential mechanisms by which AMPK activation inhibits protein synthesis. AMPK is activated in response to cellular stress via a rise in intracellular AMP concentration (LKB1 pathway) or by hyperosmolarity (probably via a rise in intracellular Ca^{2+} and the CAMKK pathway). Once activated, AMPK has been proposed to inhibit mTOR signalling and protein synthesis elongation via the activation of eEF2K which in turn phosphorylates and inactivates eEF2. A reduction in mTOR signalling could lead to an increase in eEF2 phosphorylation because eEF2K can be phosphorylated and inactivated by p70S6K. In the scheme, arrows indicate steps leading to stimulation or activation, whereas bars with a cross-head indicate steps of inhibition or inactivation.

mTOR by an as-yet-unknown mechanism. In addition, AMPK has been reported to phosphorylate mTOR at Thr2446 leading to a decrease in p70S6K activation by insulin [8]. However, under conditions of mild ATP depletion, the principal mechanism of protein synthesis inhibition probably involves AMPK-mediated eEF2 phosphorylation rather than a reduction in mTOR signalling [17,16,28]. A summary of the potential mechanisms by which AMPK activation inhibits protein synthesis is depicted in Fig. 1.

Materials and methods

Materials

Anti-human eEF2 goat polyclonal antibody was from Santa Cruz. Anti-rat/human phospho-Ser79 ACC1 peptide rabbit polyclonal antibody was from Upstate. Anti-human phospho Thr172 AMPK α-subunit, anti-human phospho Ser51 eIF2α, anti-mouse phospho Thr37/46 4E-BP1[1] and

anti-human phospho Ser235/236 S6 ribosomal protein peptide polyclonal antibodies (all raised in rabbit) were from Cell Signalling Technologies. An anti-phospho Thr56 eEF2 peptide polyclonal antibody was raised in rabbits against the phosphopeptide TRF**Tp**DTR (human, rat and mouse sequences) [26] plus an N-terminal cysteine for coupling to keyhole limpet haemocyanin. Mouse monoclonal antibodies were raised against over-expressed human p65 regulatory and p35 catalytic subunits of protein phosphatase 2A (PP2A) as described [1]. These antibodies are routinely used in the Rider Laboratory to study AMPK signalling in rat hepatocytes and rat cardiomyocytes where relevant signals are obtained in immunoblot experiments. L-[4,5-^{3}H]leucine (166 Ci/mmol) was from Amersham Biosciences (G.E. Healthcare). Other chemicals were from Sigma, Boehringer or from sources previously cited [18].

Animals

Adult male wood frogs (*R. sylvatica*) were collected in early April from meltwater ponds in Ottawa area woodlands; water temperature was 0–5 °C. Animals were rinsed in a tetracycline bath and housed at 5 °C in plastic boxes containing damp sphagnum moss for 1–2 weeks before use.

[1] *Abbreviations:* 4E-BP1; eukaryotic initiation factor 4E-binding protein-1, ACC; acetyl-CoA carboxylase (EC 6.4.1.2), AMPK; AMP-activated protein kinase, eEF2; eukaryotic elongation factor-2, eEF2K; eukaryotic elongation factor-2 kinase, mTOR; mammalian target of rapamycin, p70S6K; p70 ribosomal protein S6 kinase, S6; 40S ribosomal protein S6.

Control frogs were sampled from this condition and other frogs (*R. sylvatica*) were subjected to anoxia, dehydration, freezing, and thawing recovery treatments as described previously [29]. Experimental animals were sampled from the following conditions: control (5 °C for 1 week), anoxia (24 h under N_2 gas at 5 °C), dehydrated (40% of total body water lost at 5 °C), frozen (24 h freezing exposure at −2.5 °C), and thawed (8 h thawed at 5 °C after 24 h frozen). Frogs were sacrificed by pithing and tissues were rapidly excised, flash frozen in liquid nitrogen, transported to their destination on dry ice and then stored at −80 °C until use.

Tissue extracts

Frozen tissue samples were rapidly weighed and homogenized (Ultra-Turrax, 5×15 s) in 1:5 w/v (liver) or 1:4 w/v (skeletal muscle) of ice cold extraction buffer containing 50 mM Hepes, pH 7.4, 250 mM sucrose, 20 mM NaF, 5 mM sodium pyrophosphate, 1 mM EDTA, 1 mM EGTA, 1 mM dithiothreitol, 5 μg/ml leupeptin, 1 mM benzamidine–HCl, and 1 mM phenylmethanesulphonyl fluoride. Extracts were clarified by centrifugation (Eppendorf microfuge, full speed 15 min at 4 °C). Sample supernatants were then removed and stored at −80 °C prior to measurements of enzyme activity and immunoblotting.

AMPK assay

Sample supernatants (0.5 ml) were mixed with 0.5 ml of 20% (w/v) polyethylene glycol 8000 prepared in extraction buffer. After 30 min on ice, the samples were centrifuged (Eppendorf microfuge, full speed 1 min at 4 °C) and protein precipitates were resuspended in 0.2 ml (liver) or 0.1 ml (muscle) of extraction buffer. Polyethylene glycol fractions were diluted 1:5 (liver) and 1:3 (muscle) in extraction buffer and 2.5 μl aliquots (corresponding to about 30 μg of liver protein and about 20 μg of muscle protein) were assayed for total AMPK activity in a final volume of 30 μl containing 0.2 mM SAMS peptide, 0.2 mM AMP and 0.1 mM [γ-^{32}P]MgATP (specific radioactivity 250 cpm/pmol) at 30 °C [10]. After 5 min, up to which time the assays were linear, 10 μl aliquots were spotted onto Whatman P81 papers for the measurement of ^{32}P-incorporation [35]. One unit of enzyme activity is the amount that catalyses the phosphoryla-tion of 1 nmol of substrate under the conditions of the assay.

Immunoblotting

Equal amounts of protein sample were loaded into each well of SDS-gels as indicated in the figure legends. The percentage of acrylamide used for the gels depended on the protein under study. Acrylamide concentrations were 15% (w/v) for 4E-BP1, 12.5 % (w/v) for PP2A and ribosomal protein S6, 10% (w/v) for AMPK and eEF2 and 7.5% (w/v) for ACC. Proteins were transferred to polyvinylidine difluoride membranes (low fluorescence, GE Healthcare) and incubated in LI-COR Odyssey™ Blocking buffer for 1 h. The membranes were washed 3×10 min with TBS (10 mM Tris–HCl, pH 7.4, 0.15 M NaCl) plus Tween 20 (0.1% w/v). Membranes were incubated with various dilutions of primary antibodies in the same buffer for 2–16 h (1:1000 for anti-phospho Thr172 AMPK, 1:1000 for anti-phospho Thr56 eEF2 and full-length eEF2, 1:1000 for the anti-p35 catalytic subunit PP2A, 1:2500 for the anti-p65 regulatory subunit of PP2A and 1:1000 for the anti-phospho Ser79 ACC, anti-phospho Ser235/236 ribosomal protein S6 and anti-phospho Thr37/46 4E-BP1 antibodies). The membranes were immersed in blocking buffer containing Tween 20 (0.1% w/v) and 1 μg/ml of either secondary goat IgGs conjugated to Alexa dye 680 (Molecular Probes) or secondary rabbit or mouse IgGs coupled to IR Dye 800 (Rockland Inc.) and left shaking for 1 h protected from light. The membranes were then washed for 3×10 min using TBS–Tween (0.1% w/v). The membranes were scanned in two different channels using the Odyssey IR imager and the band intensities were quantified using the Odyssey software. Ratios of band intensities relative to signals obtained with anti-total eEF2 were calculated and normalized to the control. This had to be done to compare data obtained from the Odyssey because the blots could not all be developed with the same reagents, in parallel, on the same day and because of differences in electroblotting efficiency. In some experiments, after protein transfer to polyvinylidine difluoride membranes, blots were developed for imaging by enhanced chemi-luminescence as described previously [18].

Cell-free in vitro translation assays

Tissue extract supernatants (0.5 ml) were filtered through Sephadex G-25 columns (PD-10, Pharmacia

Biotech Ltd.) equilibrated with 50 mM Hepes pH 7.4, 200 mM potassium acetate, 5 mM magnesium acetate, 2.5 mM dithiothreitol (plus protease inhibitors, see above) to remove endogenous amino acids. For *in vitro* protein synthesis measurements, filtrates (50 µl corresponding to about 1 mg of protein) were incubated at 25 °C in a final volume of 0.1 ml of 50 mM MOPS, pH 7.1, 140 mM potassium acetate, 20 mM magnesium acetate, 2 mM dithiothreitol containing 10 M creatine phosphate, 50 µg/ml creatine phosphokinase, 1 mM ATP, 0.5 mM GTP, 0.1 mM spermidine, 10 U RNaseOUT (Invitrogen) 50 µg/ml total RNA (prepared from mouse liver [24]) and 20 µM of each of the 20 amino acids except leucine. The reactions were started by the addition of 20 µM L-[4,5-^{3}H]leucine (specific radioactivity 2000 dpm/pmol) and stopped after 90 min with 1 ml of 10% (w/v) trichloroacetic acid. After 10 min on ice, precipitated proteins were collected by centrifugation (7000 rpm × 5 min, Eppendorf microfuge), resuspended in 0.2 ml 0.1 M NaOH and re-precipitated with 1 ml of 5% (w/v) trichloroacetic acid. After 10 min on ice, proteins were collected by centrifugation and subjected to one more wash/precipitation step. Finally, precipitated proteins were solubilized in 1 ml of formic acid and 0.9 ml was taken for counting in 10 ml of scintillant (Ultima Gold, Perkin-Elmer).

Other methods

Protein concentrations were estimated [4] using human γ-globulin as a standard. Statistically significant differences were assessed using one-way analysis of variance followed by a Tukey *post hoc* test.

Results

AMPK activity and α-subunit phosphorylation

In polyethylene glycol fractions prepared from tissue extracts, AMPK activity was increased 2-fold in liver of frozen wood frogs compared with the controls and 2.5-, 4.5- and 3-fold in skeletal muscle from dehydrated, frozen and thawed animals, respectively (Fig. 2). Consistent with the increase in AMPK activity in liver during freezing, immunoblotting with an anti-phospho Thr172 α1/α2-AMPK antibody revealed an increase in T-loop phosphorylation of AMPK in liver extracts from frozen frogs (Fig. 3A). Unfortunately, we were unable to obtain meaningful blots from polyethylene glycol fractions of skeletal muscle with the anti-phospho Thr172 α1/α2-AMPK antibody because there were too many contaminating non-specific bands.
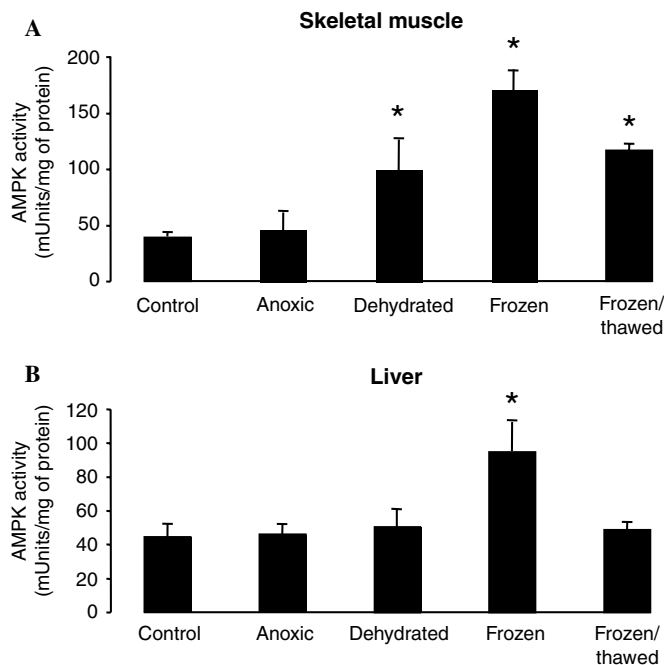

Fig. 2. AMPK activity in skeletal muscle (A) and liver (B) of stressed frogs. AMPK was assayed in polyethylene glycol fractions as described under Materials and methods. The results are the means ± SD of three individual animals subjected to each stress condition. The symbol ∗-indicates a statistically significant difference compared with the controls ($p < 0.01$).

ACC Ser79 phosphorylation

Polyethylene glycol fractions from liver and skeletal muscle extracts were immunoblotted using a commercial phosphopeptide antibody raised against the sequence "HMRSSMSGLHLVL" corresponding to the AMPK phosphorylation site (Ser79) in rat ACC1. Signals were only obtained from liver fractions (Fig. 3B) and indicated that, in parallel with AMPK activation (Figs. 2B and 3A), ACC Ser79 phosphorylation was significantly increased in the frozen condition. Meaningful blots could not be obtained from skeletal muscle, probably due to poor

recognition of the phosphorylation site in wood frog muscle ACC2 by the commercial anti-phospho Ser79 ACC1 antibody. The sequence surrounding the human ACC2 AMPK phosphorylation site (Ser221) is TMRPSMSGLHLVK, but a database search of frog genomes with this sequence failed to yield any homology.

eEF2 Thr56 phosphorylation

Frog tissue extracts were blotted with an anti-phospho Thr56 eEF2 antibody generated in our laboratory. Cross-reactivity should not have been a
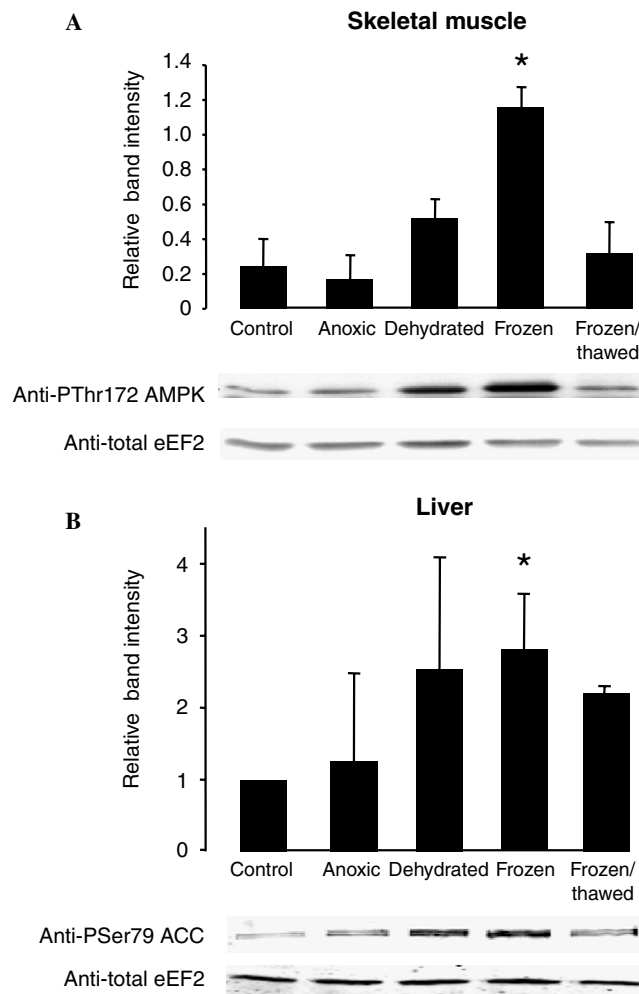

Fig. 3. Phosphorylation state of AMPK α1/α2 Thr172 (A) and ACC1 Ser79 (B) in livers of stressed frogs. Polyethylene glycol fractions (40 μg of protein in each lane) prepared from frog liver extracts were subjected to SDS–PAGE and immunoblotted with anti-phospho Thr172 AMPK (A) or anti-phospho Ser79 ACC antibody (B). The blots were developed by chemiluminescence and stripped for blotting with eEF2 as a loading control. Band intensities were quantified by scanning densitometry of films. The histograms show mean arbitrary units of phospho Thr172 AMPK (A) or anti-phospho Ser79 ACC (B) relative band intensities normalized to total eEF2 for tissues from three individuals ± SD. Representative blots are shown below the histogram. The symbol ∗-indicates a statistically significant difference compared with the controls ($p < 0.01$).

A

Skeletal muscle

Anti-PThr56 eEF2

Anti-total eEF2
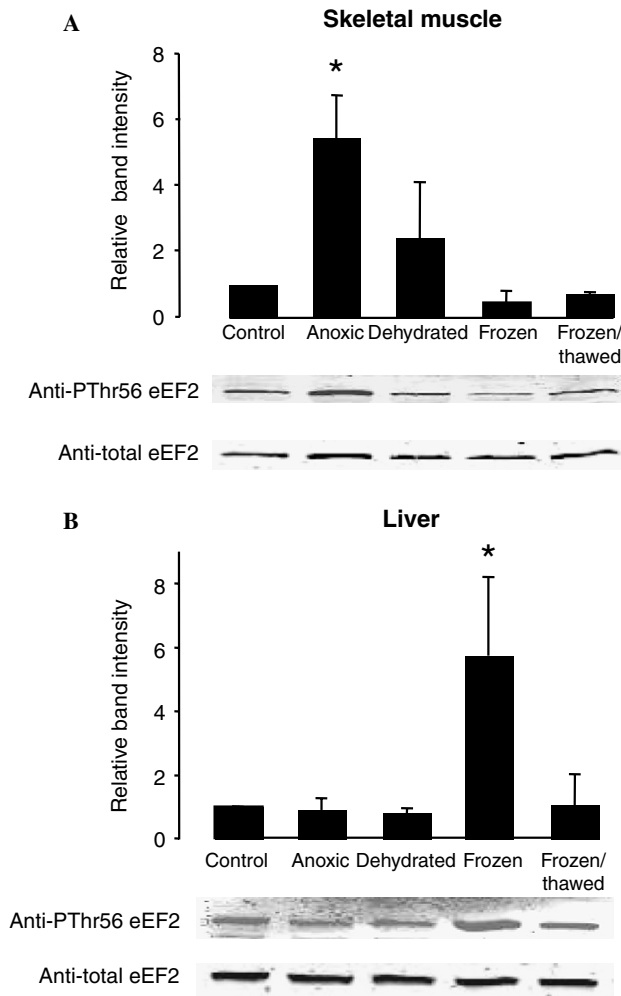
B

Liver

Anti-PThr56 eEF2

Anti-total eEF2

Fig. 4. Phosphorylation state of eEF2 Thr56 in skeletal muscle (A) and liver (B) of stressed frogs. Extracts (40 μg of protein in each lane) were subjected to SDS–PAGE and blots were probed with anti-phospho Thr56 eEF2 antibody along with anti-total eEF2 antibodies for detection with IR-conjugated secondary antibodies and quantification by Odyssey imaging. The histograms show mean arbitrary units of phospho Thr56 eEF2 relative band intensity normalized to total eEF2 and then to the control, for tissues from three individuals ± SD. Representative blots are shown below the histogram. The symbol ∗-indicates a statistically significant difference compared with the controls ($p < 0.01$).

problem since the peptide sequence to which the antibody was raised (around human eEF2 Thr56: TRF**T**DTR) is perfectly conserved in *Xenopus laevis* and *Xenopus tropicalis* (Swiss-Prot Accession Nos. Q72XP8 and Q6P3N8, respectively). Signals were readily detectable in wood frog tissues and were strongly increased by 5–6-fold both in liver from frozen frogs and in skeletal muscle from anoxic animals (Fig. 4). In all immunoblotting experiments, band intensities were calculated relative to signals obtained with anti-total eEF2 as a loading control, as in our previous work [18]. However, we first verified that total eEF2 levels were constant and unaffected by the various stresses when expressed

relative to β-actin as an alternative loading control (not shown).

eIF2α Ser51 phosphorylation

Frog tissue extracts were blotted with a commercial Ser51 eIF2α antibody. Cross-reactivity should not have been a problem since the sequence around human eIF2α Ser51 (LSEL**S**RRRIRS) is perfectly conserved in *X. tropicalis* (Swiss-Prot Accession No. Q6GL89). No change in eIF2α Ser51 phosphorylation levels in extracts of liver or skeletal muscle from stressed wood frogs was observed (data not shown).
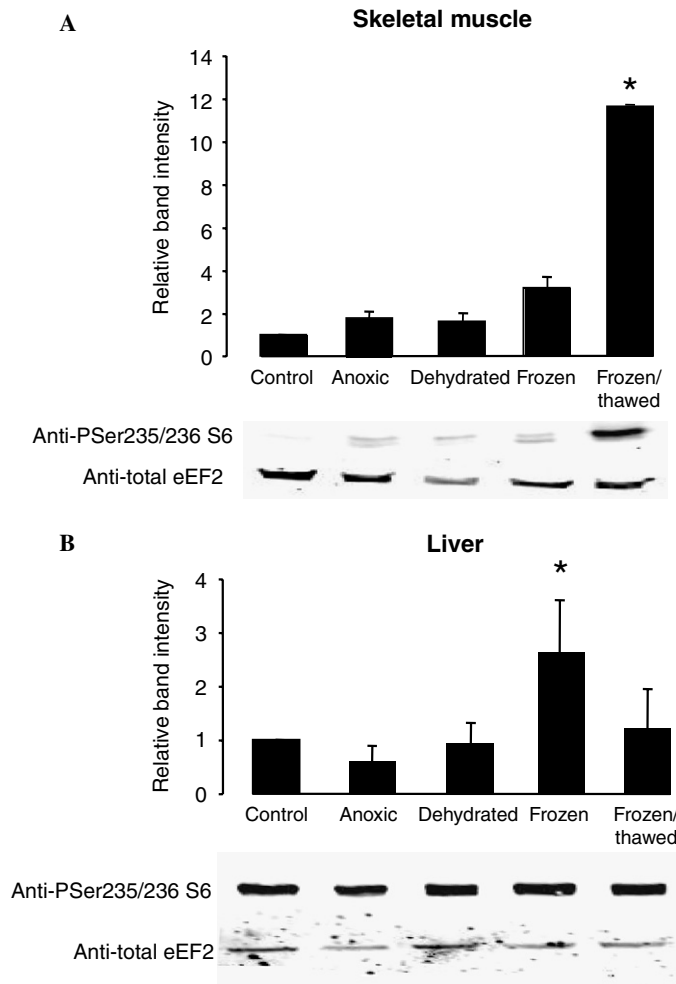
Fig. 5. Phosphorylation state of ribosomal protein S6 Ser235/236 in skeletal muscle (A) and liver (B) of stressed frogs. Extracts (40 μg of protein in each lane) were subjected to SDS–PAGE and blots were probed with anti-phospho Ser 235/236 ribosomal protein S6 antibody along with anti-total eEF2 antibodies for detection by Odyssey imaging. The histograms show mean arbitrary units of phospho Ser235/236 ribosomal protein S6 relative band intensity normalized to total eEF2 and then to the control, for tissues from three individuals ± SD. Representative blots are shown below the histogram. The symbol ∗-indicates a statistically significant difference compared with the controls ($p < 0.01$ in panel A and $p < 0.05$ in panel B).

Ribosomal protein S6 and 4E-BP1 phosphorylation

Because AMPK activation has been shown to reduce mTOR signalling, we investigated the phosphorylation state of ribosomal protein S6 and 4E-BP1, which lie downstream of mTOR, as a readout of activity of the p70S6K/mTOR pathway (Fig. 1). Frog tissue extracts were first blotted with a commercial Ser235/236 ribosomal protein S6 antibody. Cross-reactivity should not have been a problem since the sequence around Ser235/236 of human ribosomal protein S6 (KRRRLSSLRAST) is perfectly conserved in *X. laevis* (Swiss-Prot Accession No. P39017). Surprisingly, S6 phosphorylation was

increased 2.5-fold in liver from frozen frogs and almost 12-fold in skeletal muscle from frozen/thawed frogs (Figs. 5A and B). Frog tissue extracts were next blotted with a commercial Thr37/46 4E-BP1 antibody. Cross-reactivity should not have been a problem since the sequence around Thr37/46 of mouse 4E-BP1 (PPGDYST**T**PGGTLFST**T** PG) is similar in *X. laevis* (LPHDYCT**T**PGGTLFS T**T**PG, NCBI Accession No. BC075198). Interestingly, the increase in S6 phosphorylation in skeletal muscle from frozen/thawed frogs (Fig. 5A) was paralleled by an increase in 4E-BP1 phosphorylation in this condition (Fig. 6). No significant changes in 4E-BP1 phosphorylation in liver were
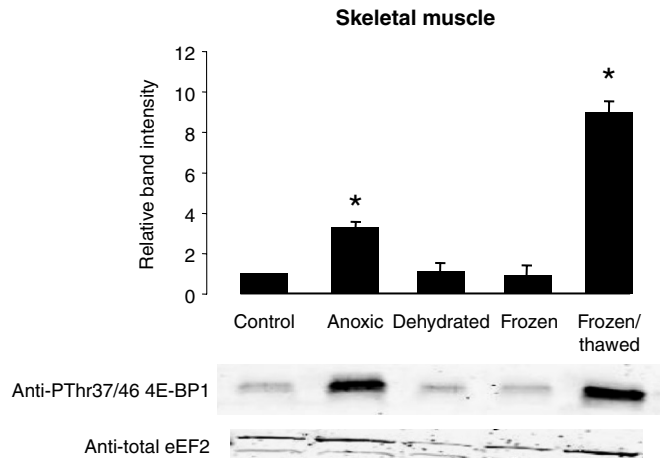
Skeletal muscle

Anti-PThr37/46 4E-BP1

Anti-total eEF2

Fig. 6. Phosphorylation state of 4E-BP1 in skeletal muscle of stressed frogs. Extracts (40 μg of protein in each lane) were subjected to SDS-PAGE and blots were probed with anti-phospho Thr37/46 4E-BP1 antibody along with anti-total eEF2 antibodies for detection by Odyssey imaging. The histogram shows mean arbitrary units of phospho Thr37/46 4E-BP1 relative band intensities normalized to total eEF2 and then to the control, for tissues from three individuals ± SD. Representative blots are shown below the histogram. The symbol ∗-indicates a statistically significant difference compared with the controls ($p < 0.01$).

observed in any of the stress conditions (not shown).

PP2A p35 catalytic and p65 regulatory subunit protein levels

Since some of the increases in the phosphorylation states of translation factors were not related to AMPK activation and could have resulted from a decrease in expression levels of PP2A, we immunoblotted the frog extracts with monoclonal antibodies raised against the PP2A p65 regulatory and p35 catalytic subunits. No significant changes in expression levels of the PP2A subunits were detected either in skeletal muscle or liver from frogs under the different stress conditions (data not shown).

Cell-free in vitro translation assays

Since the most dramatic changes in AMPK activity and the phosphorylation states of translation factors were observed in skeletal muscle, the translational capacities of filtered extracts from muscles of stressed frogs were compared by measuring rates of L-[4,5-³H]leucine incorporation into protein *in vitro* at 25 °C. However, no significant changes in protein synthesis capacity were observed in extracts from frogs subjected to the different stresses (Fig. 7).
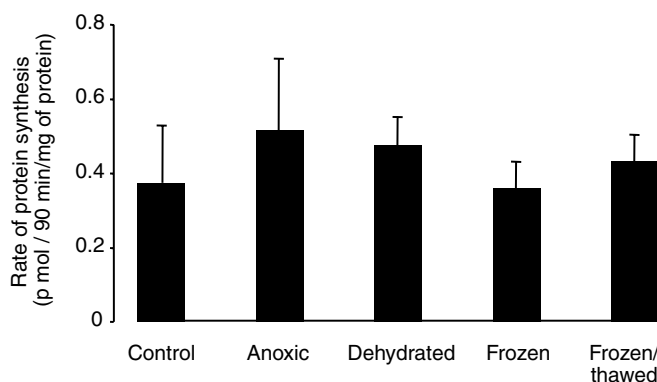

Fig. 7. Cell-free translation in skeletal muscle of stressed frogs Extracts were subjected to gel filtration to remove endogenous amino acids and were then used in cell-free translation assays as described under Materials and methods. The histogram shows mean *in vitro* protein synthesis rates for three individuals ± SD.

Discussion

Mechanisms of hypoxia/anoxia tolerance have received much attention with research focused in multiple areas including the control of energy metabolism, maintenance of membrane potential difference and ion homeostasis, regulation of energy-expensive cellular activities, and gene expression responses which are often under the control of the hypoxia-induced transcription factor (HIF). An overriding principle for survival by anoxia tolerant species is metabolic rate depression, a coordinated suppression of the rates of ATP-producing and ATP-consuming processes to achieve a new low rate of ATP turnover that can be sustained over the long-term by the ATP output from anaerobic glycolysis [42]. For example, it is well-established that protein synthesis, one of the major energy expenditures in cells, is strongly suppressed under anoxia in both vertebrates and invertebrates (e.g. 13,15). AMPK is a critical sensor of cellular energy status, yet little is known about the role that it plays in regulating cellular responses in organisms that are tolerant of long-term anoxia exposure and/or other stresses (such as freezing) that cut off oxygen supplies to tissues.

Freeze tolerance is a complex phenomenon requiring adaptive mechanisms that address multiple stresses including the ischaemia that is brought on by the freezing of blood plasma and cellular dehydration due to cell water loss into extracellular ice masses. Indeed, various metabolic and gene expression responses to freezing are known to be triggered by one of these component stresses. For example, cryoprotectant synthesis by wood frog liver can also be triggered by dehydration alone, whereas the up-regulation of several freeze responsive genes is mimicked by anoxia exposure of the animals [39,43]. For this reason, our exploration of AMPK and protein synthesis responses to freezing also analyzed the independent responses to anoxia or dehydration as well as the response to thawing after long-term freezing.

AMPK was activated by freezing in both wood frog tissues tested. Activity increased 2.5-fold in liver and 4.5-fold in muscle of frozen frogs (Fig. 2) and, in liver, the mechanism of AMPK activation was confirmed to be via phosphorylation of its T-loop Thr172 residue (Fig. 3A). AMPK activity remained high (3-fold above control) in skeletal muscle after 6 h of thawing (following 24 h frozen) but both activity and Thr172 phosphorylation state had

returned to control levels in liver within the 6 h time frame. AMPK activity in skeletal muscle also responded to dehydration, suggesting that cell volume signals may be involved in triggering AMPK activation in this tissue. AMPK stimulates glucose uptake into skeletal muscle and heart [30,36] independently of insulin. Hence, it can be postulated that at least one function of AMPK activation in muscle during freezing or dehydration (both of which trigger massive glycogenolysis and glucose export from wood frog liver) could be to stimulate glucose uptake into muscle to provide cryoprotection, although Akt/PKB activation might also be important in this respect. Glucose concentrations in tissues of frogs increase dramatically during freezing with the sugar playing a cryoprotectant role to protect/stabilize the intracellular environment during extracellular freezing [40,43].

Interestingly, a Blast search of frog sequences in the NCBI database with the rat α1 AMPK sequence gave two hits in the *X. laevis* genome with Accession Nos. BC084741 and AF340021 (the latter corresponding to Swiss-Prot Accession No. Q8UVW8). These most likely correspond to the frog orthologues of the α1 and α2 mammalian isozymes. An alignment of these frog sequences with the rat α1 and α2 AMPK sequences indicated almost complete conservation of the activation loop (T-loop) motif (not shown). Not surprisingly then, immunoblotting of liver polyethylene glycol fractions with mammalian anti-phosphoThr172 AMPK antibody revealed a significant band at the expected M_r of about 60,000 for AMPK and the band intensity increased in liver from frozen animals (Fig. 3A), in line with the increase in AMPK activity (Fig. 2B).

A well-known consequence of AMPK activation is the phosphorylation of ACC1 at the inactivating Ser79 site [14] and indeed, immunoblotting of wood frog liver extracts showed a significant 2.5-fold increase in Ser79 ACC1 phosphorylation state in frozen frogs (Fig. 3B) mirroring AMPK activation in the organ (Fig. 2B). Clearly then, fatty acid biosynthesis would be inhibited during freezing. However, the opposing AMPK-mediated stimulation of fatty acid oxidation that would normally occur in mammalian cells would not occur in these frogs due to a lack of oxygen in the frozen condition. Wood frogs have huge glycogen reserves of about 180 mg/g of liver and so the primary events during freezing would be (A) to suppress energy-consuming processes in all organs as much as possible, and (B) to trigger massive glycogenolysis and glucose export

from liver. The roles of AMPK in this situation likely include stimulating glucose uptake by non-hepatic organs, aiding glycolytic ATP production, and shutting off energy-expensive activities such as various biosynthetic pathways. Regarding the mechanism of AMPK activation during freezing, ATP and total adenylate levels were reported to be decreased in liver and muscle after 2 days of freezing in *R. sylvatica* and this was accompanied by a 2.5-fold increase in AMP [38,41] which would be expected activate AMPK via the LKB1 pathway [20]. AMPK activation in the frozen state could also be due to hyperosmolarity [49], the latter probably triggering the calmodulin-dependent kinase pathway of AMPK activation [48].

Heat shock and nutrient deprivation lead to eIF2α phosphorylation at the inactivating Ser51 site and in mammals four eIF2α kinases are known. In desert frogs during estivation [31] and in anoxic snails [23], protein synthesis was shown to be down-regulated and under these conditions, eIF2α Ser51 phosphorylation increased. However, in this study we detected no changes in eIF2α phosphorylation state in response to the stresses in skeletal muscle and liver of *R. sylvatica*. Hence, freeze-responsive regulation of protein synthesis may occur through a different mechanism such as control via eEF2 phosphorylation to down-regulate translation elongation.

It was previously reported that anoxia exposure of frogs (*Rana perezi*) increased liver AMPK Thr172 phosphorylation 4-fold and increased eEF2 Thr56 phosphorylation levels by 50% [2]. In our study, eEF2 Thr56 phosphorylation increased 5–6-fold in liver from frozen frogs (Fig. 4B) but no significant increase in AMPK activity (Fig. 2B) or eEF2 phosphorylation was seen in liver during anoxia (Fig. 4B). However, there was an increase in eEF2 phosphorylation (5–6-fold) in skeletal muscle of anoxic wood frogs (Fig. 4A). During freezing in the liver, AMPK activation could be responsible for the rise in eEF2 phosphorylation and this would be expected to inhibit protein synthesis by decreasing peptide chain elongation. A rise in intracellular Ca^{2+} as a result of an increase in hyperosmolarity following freezing could also be responsible for the increase in eEF2 phosphorylation in this condition, as eEF2K is stimulated by Ca^{2+}/calmodulin (Fig. 1) [6]. However, in liver from dehydrated frogs where an increase in hyperosmolarity might also be expected, there was no increase in eEF2 phosphorylation state compared with the controls (Fig. 4B). In skeletal muscle during

anoxia, mechanism(s) other than via AMPK activation must be responsible for the rise in eEF2 phosphorylation, since AMPK was not activated in this condition (Fig. 2A). A reduction in mTOR signalling was not evident, as there was no decrease in muscle ribosomal S6 or 4E-BP1 phosphorylation (Figs. 5A and 6), and expression levels of the catalytic and regulatory subunits of PP2A, which dephosphorylates eEF2 [33], were unchanged in skeletal muscle from anoxic frogs (not shown). This correlates with the results from direct measurements of PP2A activity in wood frog skeletal muscle which showed a small increase (25% between 5 and 20 min) in PP2A activity just after freezing started, but this reverted to control levels after longer freezing (1 and 8 h) [25].

AMPK was activated in liver of frozen frogs and in skeletal muscle of frozen–thawed frogs, which would be expected to reduce mTOR signalling under these conditions (Fig. 1). Surprisingly, ribosomal S6 phosphorylation increased 2.5-fold in liver of frozen frogs (Fig. 5B) and almost 12-fold in skeletal muscle of frozen/thawed wood frogs (Fig. 5A). Moreover, the increase in ribosomal S6 phosphorylation (Fig. 5A) was paralleled by a rise in 4E-BP1 phosphorylation (Fig. 6) in skeletal muscle from frozen/thawed frogs. Therefore, mechanisms must exist to override the AMPK-induced inhibition of mTOR signalling under certain conditions. Paradoxically, the increases in ribosomal protein S6 and 4E-BP1 phosphorylation would be expected to stimulate protein synthesis in liver of frozen frogs and in skeletal muscle of frozen/thawed animals. p70S6K phosphorylates Ser235/Ser236 of the 40S ribosomal S6 protein and this is thought to be important for cell growth [32]. p70S6K and ribosomal protein S6 phosphorylation do not seem to be necessary for the translation of terminal oligopyrimidine tract (TOP) mRNAs [37] which encode components of the protein synthesis machinery (see however [34]). mTOR phosphorylates Thr37/Thr46 of 4E-BP1 which relieves the inhibition of eIF-4E to allow the initiation of capped mRNAs to proceed [32]. The increases in ribosomal protein S6 and 4E-BP1 phosphorylation might be required for the synthesis of a subset of proteins [45] under conditions in which global translation would be decreased. For example, a variety of genes have been identified as freeze responsive in wood frog liver from cDNA library or cDNA array screening, three of these being freeze-specific novel genes, and follow-up studies of some of these genes have also confirmed an associated increase in protein (summarized in [39]).

To directly determine if the capacity of protein synthesis was altered under freezing, anoxia or dehydration stresses, we monitored cell-free translation in skeletal muscle extracts of the stressed frogs. However, no changes in overall protein synthesis rates *in vitro* were observed in any of the conditions (Fig. 7). One could argue that stable changes in the translational machinery might not have persisted since protein phosphatase inhibitors were not included in the buffer for gel filtration (to remove endogenous amino acids from the extracts). However, fluoride has been reported to be inhibitory to cell free translation [9]. Importantly, the effect of anoxia on protein synthesis in brine shrimp embryos was found to persist during cell-free translation measurements when extracts were prepared without fluoride [15]. The lack of any changes in overall cell-free protein synthesis rates in muscles from stressed frogs is perhaps not surprising. The frogs did not eat during the study and it is likely that protein synthesis was already down-regulated in control animals. It is noteworthy in this respect that the immunoblots indicate signals for phospho-eEF2 and phospho-eIF2α that were appreciable in the controls.

In conclusion, AMPK activation in liver of frozen frogs and in skeletal muscle of dehydrated, frozen and frozen–thawed wood frogs could be involved in inhibiting energy consuming pathways. In the frozen state, AMPK activation in liver could facilitate glycogen mobilization for glucose cryoprotectant release by inhibiting glycogen synthase activity while in skeletal muscle (and likely other organs as well) AMPK activation could stimulate glucose uptake for cryoprotection. In skeletal muscle, there was no correlation between AMPK activation and eEF2 phosphorylation but in liver, AMPK activation could be responsible for the increase in eEF2 phosphorylation and hence an inhibition of protein synthesis during freezing. The increase in ribosomal protein S6 and 4E-BP1 phosphorylation in skeletal muscle of anoxic and frozen–thawed frogs could be important for priming translation initiation or be necessary for the synthesis of a subset of proteins required for adaptation to these conditions.

References

[1] D. Abraham, K. Podar, M. Pacher, M. Kubicek, N. Welzel, B.A. Hemmings, S.M. Dilworth, H. Mischak, W. Kolch, M. Baccarini, Raf-1-associated protein phosphatase 2A as a positive regulator of kinase activation, J. Biol. Chem. 275 (2000) 22300–22304.

[2] M. Bartrons, E. Ortega, M. Obach, M. N Calvo, A. Navarro-Sabate, R. Bartrons, Activation of AMP-dependent protein kinase by hypoxia and hypothermia in the liver of frog *Rana perezi*, Cryobiology 49 (2004) 190–194.

[3] D.R. Bolster, S.J. Crozier, S.R. Kimball, L.S. Jefferson, AMP-activated protein kinase suppresses protein synthesis in rat skeletal muscle through downregulated mTOR signalling, J. Biol. Chem. 277 (2002) 23977–23980.

[4] M.M. Bradford, A rapid and sensitive method for the quantitation of microgram quantities of protein utilizing the principle of protein–dye binding, Anal. Biochem. 72 (1976) 248–254.

[5] G.J. Browne, S.G. Finn, C.G. Proud, Stimulation of the AMP-activated protein kinase leads to activation of eukaryotic elongation factor 2 kinase and to its phosphorylation at a novel site, serine 398, J. Biol. Chem. 279 (2004) 12220–12231.

[6] G.J. Browne, C.G. Proud, Regulation of peptide-chain elongation in mammalian cells, Eur. J. Biochem. 269 (2002) 5360–5368.

[7] F. Buttgereit, M.D. Brand, A hierarchy of ATP-consuming processes in mammalian cells, Biochem. J. 312 (1995) 163–167.

[8] S.W.Y. Cheng, L.G.D. Fryer, D. Carling, P.R. Shepherd, T2446 is a novel mTOR phosphorylation site regulated by nutrient status, J. Biol. Chem. 279 (2004) 15719–15722.

[9] J.W. Cosgrove, S.I. Rapoport, Absence of age differences in protein synthesis by rat brain, measured with an initiating cell-free system, Neurobiol. Aging 8 (1987) 27–34.

[10] S.P. Davies, D. Carling, D.G. Hardie, Tissue distribution of the AMP-activated protein kinase, and lack of activation by cyclic-AMP-dependent protein kinase, studied using a specific and sensitive peptide assay, Eur. J. Biochem. 186 (1989) 123–128.

[11] P.B. Dennis, A. Jaeschke, M. Saitoh, B. Fowler, S.C. Kozma, G. Thomas, Mammalian TOR: A homeostatic ATP sensor, Science 294 (2001) 1102–1105.

[12] P.F. Dubbelhuis, A.J. Meijer, Hepatic amino acid-dependent signaling is under control of AMP-dependent protein kinase, FEBS Lett. 521 (2002) 39–42.

[13] K.P. Fraser, D.F. Houlihan, P.L. Lutz, S. Leone-Kabler, L. Manuel, J.G. Brechin, Complete suppression of protein synthesis during anoxia with no post-anoxia protein synthesis debt in the red-eared slider turtle *Trachemys scripta elegans*, J. Exp. Biol. 204 (2001) 4353–4560.

[14] D.G. Hardie, D. Carling, M. Carlson, The AMP-activated/SNF1 protein kinase subfamily: metabolic sensors of the eukaryotic cell? Annu. Rev. Biochem. 67 (1998) 821–855.

[15] G.E. Hofmann, S.C. Hand, Global arrest of translation during invertebrate quiescence, Proc. Natl. Acad. Sci. USA 91 (1994) 8492–8496.

[16] S. Horman, C. Beauloye, D. Vertommen, J.-L. Vanovers-chelde, L. Hue, M.H. Rider, Myocardial ischemia and increased heart work modulate the phosphorylation state of eukaryotic elongation factor-2, J. Biol. Chem. 278 (2003) 41970–41976.

[17] S. Horman, G.J. Browne, U. Krause, J.V. Patel, D. Vertommen, L. Bertrand, A. Lavoine, L. Hue, C.G. Proud, M.H. Rider, Activation of AMP-activated protein kinase leads to the phosphorylation of elongation factor 2 and an inhibition of protein synthesis, Curr. Biol. 12 (2002) 1419–1423.

[18] S. Horman, N. Hussain, S.M. Dilworth, K.B. Storey, M.H. Rider, Evaluation of the role of AMP-activated protein

kinase and its downstream targets in mammalian hibernation, Comp. Biochem. Physiol. B 142 (2005) 374–382.

[19] K. Inoki, T. Zhu, K.-L. Guan, TSC2 mediates cellular energy response to control cell growth and survival, Cell 115 (2003) 577–590.

[20] B.B. Kahn, T. Alquier, D. Carling, D.G. Hardie, AMP-activated protein kinase: ancient energy gauge provides clues to modern understanding of metabolism, Cell Metab. 1 (2005) 5–25.

[21] B.E. Kemp, K.I. Mitchelhill, D. Stapleton, B.J. Michell, Z.P. Chen, L.A. Witters, Dealing with energy demand: the AMP-activated protein kinase, Trends Biochem. Sci. 24 (1999) 22–25.

[22] U. Krause, L. Bertrand, L. Hue, Control of p70 ribosomal protein S6 kinase and acetyl-CoA carboxylase by AMP-activated protein kinase and protein phosphatases in isolated cardiomyocytes, Eur. J. Biochem. 269 (2002) 3751–3759.

[23] K. Larade, K.B. Storey, Reversible suppression of protein synthesis in concert with polysome disaggregation during anoxia exposure in *Littorina littorea*, Mol. Cell. Biochem. 232 (2002) 121–127.

[24] P.M. Lizardi, Methods for the preparation of messenger RNA, Methods Enzymol. 96 (1983) 24–38.

[25] J.A. MacDonald, K.B. Storey, Protein phosphatase responses during freezing and thawing in wood frogs: control of liver cryoprotectant metabolism, Cryo-Letters 20 (1999) 297–306.

[26] P. Marin, K.L. Nastiuk, N. Daniel, J. Girault, A.J. Czernik, J. Glowinski, A.C. Nairn, J. Premont, Glutamate-dependent phosphorylation of elongation factor-2 and inhibition of protein synthesis in neurons, J. Neurosci. 17 (1997) 3445–3454.

[27] A.S. Marsin, L. Bertrand, M.H. Rider, J. Deprez, C. Beauloye, M.F. Vincent, G. Van den Berghe, D. Carling, L. Hue, Phosphorylation and activation of heart PFK-2 by AMPK has a role in the stimulation of glycolysis during ischaemia, Curr. Biol. 10 (2000) 1247–1255.

[28] L.E. McLeod, C.G. Proud, ATP depletion increases phosphorylation of elongation factor eEF2 in adult cardiomyocytes independently of inhibition of mTOR signalling, FEBS Lett. 531 (2002) 448–452.

[29] J.D. McNally, C.M. Sturgeon, K.B. Storey, Freeze-induced expression of a novel gene, fr47, in the liver of the freeze-tolerant wood frog, *Rana sylvatica*, Biochem. Biophys. Acta. 1625 (2003) 183–191.

[30] G.F. Merrill, E.J. Kurth, D.G. Hardie, W.W. Winder, AICA riboside increases AMP-activated protein kinase, fatty acid oxidation, and glucose uptake in rat muscle, Am. J. Physiol. 273 (1997) E1107–E1112.

[31] J.L. Pakay, A.A. Hobbs, S.R. Kimball, M. Guppy, The role of eukaryotic initiation factor 2alpha during the metabolic depression associated with estivation, J. Exp. Biol. 206 (2003) 2363–2371.

[32] C.G. Proud, Regulation of mammalian translation factors by nutrients, Eur. J. Biochem. 269 (2002) 5338–5349.

[33] N.T. Redpath, C.G. Proud, Activity of protein phosphatases against initiation factor-2 and elongation factor-2, Biochem. J. 272 (1990) 175–180.

[34] A.K. Reiter, T.G. Anthony, J.C. Anthony, L.S. Jefferson, S.R. Kimball, The mTOR signaling pathway mediates control of

ribosomal protein mRNA translation in liver, Int. J. Biochem. Cell Biol. 36 (2004) 2169–2179.

[35] R. Roskoski Jr., Assays of protein kinase, Methods Enzymol. 99 (1983) 3–6.

[36] R. R. Russell, R. Bergeron, G.I. Shulman, L.H. Young, Translocation of myocardial GLUT-4 and increased glucose uptake through activation of AMPK by AICAR, Am. J. Physiol. 277 (1999) H643–H649.

[37] M. Stolovich, H. Tang, E. Hornstein, G. Levy, R. Cohen, S.S. Bae, M.J. Birnbaum, O. Meyuhas, Transduction of growth or mitogenic signals into translational activation of TOP mRNAs is fully reliant on the phosphatidylinositol 3-kinase-mediated pathway but requires neither S6K1 nor rpS6 phosphorylation, Mol. Cell. Biol. 22 (2002) 8101–8113.

[38] K.B. Storey, Organ-specific metabolism during freezing and thawing in a freeze tolerant frog, Am. J. Physiol. 253 (1987) R292–R297.

[39] K.B. Storey, Strategies for exploration of freeze responsive gene expression: advances in vertebrate freeze tolerance, Cryobiology 48 (2004) 134–145.

[40] K.B. Storey, Reptile freeze tolerance: Metabolism and gene expression, Cryobiology 52 (2006) 1–16.

[41] K.B. Storey, J.M. Storey, Biochemical adaptation for freezing tolerance in the wood frog, *Rana sylvatica*, J. Comp. Physiol. B 155 (1984) 29–36.

[42] K.B. Storey, J.M. Storey, Metabolic rate depression in animals: transcriptional and translational controls, Biol. Rev. Camb. Philos. Soc. 79 (2004) 207–233.

[43] K.B. Storey, J.M. Storey, Physiology, biochemistry and molecular biology of vertebrate freeze tolerance: the wood frog, in: E. Benson, B. Fuller, N. Lane (Eds.), Life in the Frozen State, CRC Press, Boca Raton, 2004, pp. 243–274.

[44] X. Wang, W. Li, M. Williams, N. Terada, D.R. Alessi, C.G. Proud, Regulation of elongation factor 2 kinase by p90[RSK1] and p70S6 kinase, EMBO J. 20 (2001) 4370–4379.

[45] D. White, K.B. Storey, Freeze-induced alterations of translatable mRNA populations in wood frog organs, Cryobiology 38 (1999) 353–362.

[46] W. Wieser, G. Krumschnabe, Hierarchies of ATP-consuming processes: direct compared with indirect measurements, and comparative aspects, Biochem. J. 355 (2001) 389–395.

[47] L.A. Witters, B.E. Kemp, A.R. Means, Chutes and Ladders: the search for protein kinases that act on AMPK, Trends Biochem. Sci. 31 (2006) 13–16.

[48] A. Woods, K. Dickerson, R. Heath, S.P. Hong, M. Momcilovic, S.R. Johnstone, M. Carlson, D. Carling, Ca^{2+}/calmodulin-dependent protein kinase kinase-beta acts upstream of AMP-activated protein kinase in mammalian cells, Cell Metab. 1 (2005) 21–33.

[49] A. Woods, D. Vertommen, D. Neumann, R. Türk, J. Bayliss, U. Schlattner, T. Wallimann, D. Carling, M.H. Rider, Identification of phosphorylation sites in AMP-activated protein kinase (AMPK) for upstream AMPK kinases and study of their roles by site-directed mutagenesis, J. Biol. Chem. 278 (2003) 28434–28442.